

Submitted to Journal of Applied Physics

LBL-3160
Preprint c.1

A LIMITING CONFIGURATION IN DISLOCATION GLIDE
THROUGH A RANDOM ARRAY OF POINT OBSTACLES

Kenton Hanson and J. W. Morris, Jr.

August 1974

Prepared for the U. S. Atomic Energy Commission
under Contract W-7405-ENG-48

For Reference

Not to be taken from this room



LBL-3160
c.1

DISCLAIMER

This document was prepared as an account of work sponsored by the United States Government. While this document is believed to contain correct information, neither the United States Government nor any agency thereof, nor the Regents of the University of California, nor any of their employees, makes any warranty, express or implied, or assumes any legal responsibility for the accuracy, completeness, or usefulness of any information, apparatus, product, or process disclosed, or represents that its use would not infringe privately owned rights. Reference herein to any specific commercial product, process, or service by its trade name, trademark, manufacturer, or otherwise, does not necessarily constitute or imply its endorsement, recommendation, or favoring by the United States Government or any agency thereof, or the Regents of the University of California. The views and opinions of authors expressed herein do not necessarily state or reflect those of the United States Government or any agency thereof or the Regents of the University of California.

A LIMITING CONFIGURATION IN DISLOCATION GLIDE THROUGH
A RANDOM ARRAY OF POINT OBSTACLES

Kenton Hanson and J. W. Morris, Jr.

Department of Materials Science and Engineering, University of
California and Inorganic Materials Research Division, Lawrence
Berkeley Laboratory, Berkeley, California 94720

ABSTRACT

We consider a dislocation in glide through a random array of point obstacles. Several important phenomena, including the critical resolved shear stress at zero temperature and the velocity of thermally activated glide at low temperature or at stress near the critical resolved shear stress, are known to be strongly influenced by the properties of the most stable obstacle configuration encountered by the dislocation during glide. We devise a limiting technique to estimate the mechanical strength, the distribution of forces, and the mean dislocation segment length in this configuration. The estimates are in good agreement with results obtained from computer-simulated glide through an array of 10^4 points.

I. INTRODUCTION

As in the earlier papers of this series¹⁻³ we consider the planar glide of a dislocation, idealized as a flexible, extensible string of constant line tension, through a random array of identical, immobile obstacles which act as point barriers to dislocation glide. In the following we develop formulae which are useful in approximating the properties of the most stable configuration which the dislocation can assume during glide through the obstacle array at a given value of the resolved shear stress. The properties of these most stable configurations are central to a theory of dislocation glide since they determine the critical resolved shear stress for planar glide at zero temperature and have a dominant influence on the velocity of thermally activated glide when the temperature is small or when the resolved shear stress is close to its critical value.

The assumptions and basic equations used below are specializations of those introduced in ref. 1. The glide plane of the dislocation is taken to be a square containing a random (Poisson) distribution of point obstacles whose density is given by the mean area (a) per point or by the characteristic length $\lambda_s = a^{1/2}$. The area of the array may be written in dimensionless form: $A^* = A/a = n$, where n is the expected number of obstacles contained. The dislocation is modeled as a flexible, extensible string of constant line tension, Γ , with Burgers vector, b , of magnitude b , in the glide plane. The resolved shear stress (τ) impelling glide may be written in dimensionless form:

$$\tau^* = \tau \lambda_s b / 2\Gamma \quad (1.1)$$

Let the dislocation, under the applied stress τ^* , encounter a configuration of point obstacles denoted by i (Fig. 1). Between two adjacent obstacles the dislocation will take the form of a circular arc of dimensionless radius $R^* (= 1/2\tau^*)$. If the distance between any two adjacent obstacles along i exceeds $2R^*$ or if the dislocation line anywhere intersects itself then configuration i is transparent to the dislocation and will be mechanically bypassed. If i is not transparent its mechanical stability is governed by the strength of the dislocation-obstacle interaction.

At the k^{th} obstacle on i the dislocation line forms the asymptotic angle ψ_i^k ($0 \leq \psi_i^k \leq \pi$). The force, F_i^k , that the dislocation exerts on the k^{th} obstacle is, in dimensionless form,²

$$\beta_i^k = F_i^k / 2\Gamma = \cos\left(\frac{1}{2}\psi_i^k\right) \quad (1.2)$$

whence $0 \leq \beta_i^k \leq 1$. The mechanical strength of the obstacle is measured by the dimensionless parameter β_c (or angle ψ_c) and corresponds to the maximum force the obstacle can sustain without being cut or locally bypassed. A nontransparent line configuration of obstacles constitutes a mechanically stable barrier to the glide of a dislocation under stress τ^* if $\beta_i^k < \beta_c$ for all obstacles k on i , hence if $\beta_i < \beta_c$ where β_i is the maximum of the β_i^k .

As is discussed in ref. 1, the set of nontransparent obstacle configurations within a given array of obstacles is uniquely determined by the dimensionless applied stress, τ^* , which fixes the dimensionless bow-out radius, R^* , of the arc of dislocation line connecting adjacent obstacles. The mechanical stability of the i^{th} of these configurations

is characterized by the maximum, β_1 , of the forces exerted on it by the dislocation. Let the β_1 be ordered in an increasing sequence. Then β_1 , the minimum of the β_1 , characterizes the configuration of greatest mechanical stability. β_1 is determined by τ^* and may easily be seen to be a monotonically increasing function of τ^* . The form of the function, as determined by computer simulation, is shown in ref. 3.

The function $\beta_1(\tau^*)$ (or, equivalently, its inverse $\tau^*(\beta_1)$) specifies the critical resolved shear stress for athermal glide through an array of obstacles of strength β_c . When $\beta_1 < \beta_c$ the dislocation will be pinned by at least one obstacle configuration within the array which must be passed by thermal activation. Hence when $\beta_1(\tau^*) = \beta_c$, $\tau^* = \tau_c^*$.

The set $\{\beta_1^k\}$ contains the forces exerted on the most stable configuration. When the number of obstacles N_1 in configuration 1 is large we assume that the distribution of forces may be represented by a normalized density function, $\rho_1(\beta, \tau^*)$, such that the number of obstacles having β_1^k in the range $\beta, \beta+d\beta$ is $N_1 \rho(\beta, \tau^*) d\beta$, with $\rho(\beta, \tau^*) = 0$ when $\beta > \beta_1(\tau^*)$. The form of the function $\rho(\beta, \tau^*)$ has been determined by computer simulation, and is given in ref. 3.

The distribution of forces along the most stable configuration strongly influences the velocity of thermally activated glide at high stress ($\tau^* \sim \tau_c^*$) or low temperature.³ In either case the velocity of glide is largely determined by the expected residence time of the dislocation in its most stable configuration. This residence time is a function of the distribution of forces.¹

In the current literature the most stable configuration is often approximated by a simple model proposed by Friedel⁴ to treat thermally

activated glide at high temperature and low stress. Fleischer and Hibbard⁵ suggested that the same model might be applied to the strength determining configuration in low-temperature glide at low stress. The pinning configuration is approximated by a straight line of equispaced points whose separation is determined by the condition that the dislocation sweep through a dimensionless area (A^*) equal to one in cutting an obstacle. The model yields, in our notation:

$$\beta_1 = (\tau^*)^{2/3}, \quad (1.3)$$

$$\rho_1(\beta; \tau^*) = \delta(\beta - \beta_1), \quad (1.4)$$

$$l^* = (\tau^*)^{-1/3}. \quad (1.5)$$

where l^* is the separation between adjacent obstacles, $\delta(x)$ is the Dirac delta function, and τ^* is assumed small.

The utility of the Friedel model was confirmed by the computer simulation experiments of Foreman and Makin⁶ who determined the critical stress for athermal glide (τ_c^*) as a function of obstacle strength (β_c) for random arrays of up to 4×10^4 points. They found that the inverse of equation (1.3) is a good approximation when the obstacle strength is small. However, a more detailed examination³ of the most stable configurations encountered in computer simulated glide revealed that the assumptions of the Friedel model are not satisfied. The most stable configuration does not tend toward a straight line of a equispaced points at low stress. It retains a β -distribution which differs qualitatively from that predicted by Eq. (1.4) and has a mean segment length appreciably below that predicted by Eq. (1.5).

To fully correct the simple Friedel model would require an exact treatment of the most stable configurations. For reasons discussed below, the formulation of an exact treatment is likely to prove a difficult task. We have, however, found an analytic technique for constructing a limiting configuration which is at least as stable as the most stable configuration in an array of arbitrarily large size. This limiting approach leads to equations for $\beta_1(\tau^*)$, $\rho_1(\beta; \tau^*)$ and $\langle \ell^* \rangle$ which are in reasonable agreement with the results of computer simulation experiments when the obstacle strength (β_c) is less than about 0.7. The technique and its consequences are developed below.

II. AN UPPER BOUND ON THE MOST STABLE CONFIGURATION

A. The Circle-Rolling Technique as a Branching Process

A useful device for locating the stable configurations within a random array of point obstacles is the "circle-rolling" technique described in reference 3. The dislocation line between two obstacles (say, $k-1$ and k) is the arc of a circle of dimensionless radius $R^* = 1/(2\tau^*)$ of strength β_c . If $k-1$ and k are obstacles in a stable configuration at τ^* then there must be at least one obstacle ($k+1$) in the area swept out by rotating the circle counter-clockwise about k through an angle

$$\theta_c = \pi - \psi_c = 2 \sin^{-1}(\beta_c) \quad (2.1)$$

Since this requirement holds for all obstacles on a stable line, the line may be generated by successive circle-rolling.

If $\tau^* < \tau_c^*(\beta_c)$ then it must be possible to locate at least one stable configuration by circle rolling. Hence, given θ_c , if there is a τ_0^* such that this technique demonstrably cannot yield a stable configuration then $\tau_0^* \geq \tau_c^*$ and is a valid upper bound. We find a τ_0^* by noting the formal similarity between the circle rolling procedure and the classical branching process in probability theory.

The classical branching process⁷ contains independent events which may produce descendants of like kind, with the number of offspring given by an integer random variable of known distribution. The theory of branching processes estimates the size of the k^{th} generation descended from a single initial event. The asymptotic size of the descendent population is sharply constrained by the extinction theorem of branching processes, which states that if $\langle n \rangle \leq 1$, where $\langle n \rangle$ is the expected

number of offspring, then the line of descent will necessarily terminate after a finite number of generations.

The circle-rolling technique locates stable configurations through a type of branching process. Let the initial or zeroth segment on a configuration be that connecting an obstacle to the left hand boundary of the array. Then the first segment, if it exists, will connect the first obstacle (1) to a second (2) located in the area (A^*) swept by rotating a circle of radius R^* through an angle θ_c about (1). Each obstacle in A^* defines a possible first segment. Since A^* is a subarea of an array containing a unit density of Poisson-distributed obstacles the probability that there are exactly ν first segments (offspring) is

$$p(\nu; A^*) = \frac{(A^*)^\nu}{\nu!} e^{-A^*} \quad (2.2)$$

The expected number of descendents in the first generation is

$$\langle n \rangle = A^* \quad (2.3)$$

Generalizing, the k^{th} segment connects the k^{th} to the $(k+1)^{\text{th}}$ obstacle along the dislocation line. The possible k^{th} segments of a configuration are the segments which can be successfully found through sequential searches by circle rolling from the initial segment; they belong to the k^{th} generation of descent from (1). Each member of each generation has descendents whose number is governed by $p(\nu; A^*)$ with expectation A^* . A given initial segment is on a stable configuration only if it has descendents through a sufficient number of generations to reach across the array. The extinction theorem may be invoked, and states that stable configurations cannot exist in an array of arbitrarily large size if

$$A^* \leq 1. \quad (2.4)$$

If the circle-rolling technique were a classical branching process the inequality (2.4) would directly yield the critical stress ($\tau_c^*(\beta_c)$) for an array of arbitrarily large size. However, the circle-rolling technique violates the assumptions of the classical branching process in two ways. First, the descendent segments found by circle-rolling are not always distinct. A particular segment may be obtainable from a given initial segment through more than one path. Second, the descendent segments are not always legitimate extensions of the dislocation line. The circle-rolling may find segments which cause the dislocation line to intersect itself and hence violate a necessary condition for mechanical stability. Both these factors reduce the number of valid dislocation segments in the k^{th} generation below the value estimated by the theory of classical branching processes. The inequality (2.4) still applies, but may be shown to yield a serious overestimate of τ_c^* . We obtain a more accurate estimate by modifying the circle-rolling procedure.

B. The Limiting Configuration Obtained Through Circle Rolling

Let a circle of radius R^* be rotated counter-clockwise through an angle θ_c about obstacle k . The new area (A^*) swept during this operation is shown in Fig. 2. The area may be described by coordinates θ and ϕ . The lines of constant θ are concave arcs generated by the leading edge of the circle as it is rotated. We choose θ such that $0 \leq \theta \leq \theta_c$ in A^* . The lines of constant ϕ are convex arcs generated by the trailing edge of the circle as it is rotated through an angle

$\pi + \theta_c$. We choose ϕ such that $-\pi \leq \phi \leq \theta_c$ in A^* .

The advantage of this parametrization of the search area is the following. Let a point $k+1$ be found at (θ, ϕ) within A^* (Fig. 3). Then θ is the angle of rotation between arcs $k-1$ and k at point k . Let \underline{t}_k be a unit tangent vector to arc $k-1$ at point k and let \underline{t}_{k+1} be a unit tangent vector to arc k at point $k+1$. Then ϕ gives the angle between \underline{t}_k and \underline{t}_{k+1} . If we now let a dislocation configuration (1) be generated by circle-rolling left to right then the angle at the k^{th} obstacle is θ_i^k and the direction of the line at the k^{th} obstacle is specified by the accumulated value of ϕ according to the relation

$$\underline{t}_k = \underline{t}_0 \exp i \left[\sum_{j=1}^k \phi_i^j \right] \quad (2.5)$$

where \underline{t}_0 is a unit vector perpendicular to the left-hand edge of the array and the imaginary axis is taken parallel to the left hand edge of the array.

Equation (2.5) yields an important constraint on a stable configuration. If a stable configuration is to connect the sides of an array of arbitrarily large size then it is necessary that

$$\langle \phi \rangle_i = \frac{1}{N_i} \sum_{k=1}^{N_i} \phi_i^k = 0. \quad (2.6)$$

where N_i is the number of obstacles in the configuration. Equation (2.6) is a weak phrasing of the constraint that a stable dislocation line cannot loop onto itself. It is clearly insufficient, since $\langle \phi \rangle = 0$ on an arbitrarily long line containing a finite number of loops and also on a line containing equal numbers of loops of positive and negative sense.

We employ the constraint (2.6) along with the extinction theorem of branching processes to establish a $\tau_o^* \geq \tau_c^*(\theta_c)$ for an array of arbitrarily large size. Given an obstacle strength (θ_c) let a configuration be generated by circle-rolling left to right. We assume a stochastic process, ignoring any illegitimacy or redundancy in descendent segments. Then in each generation the points within the search area A^* give possible extensions of the line. These points may only be used in sets which satisfy Eq. (2.6). Let $f(\theta, \phi)$, $0 \leq f \leq 1$, be the normalized frequency with which a point found at (θ, ϕ) is used to test the continuation of the line. We choose $f(\theta, \phi)$ to find the minimum value of R^* for which the circle rolling procedure will not necessarily fail.

Since each search area A^* is a sub-area of an array having a unit density of Poisson-distributed points, the probability that a point will be found in an element dA^* of A^* is simply dA^* . In terms of the coordinates (θ, ϕ) ,

$$\begin{aligned} dA^* &= R^{*2} \sin(\theta - \phi) \, d\phi d\theta \\ &= R^{*2} \, da(\theta, \phi) \end{aligned} \quad (2.7)$$

where $da(\theta, \phi)$ is independent of the radius. Given $f(\theta, \phi)$, the expected number of descendents in A^* is

$$\langle n \rangle = (R^*)^2 \iint_a f(\theta, \phi) \, da(\theta, \phi) \quad (2.8)$$

and the expected value of the coordinate ϕ is

$$\langle \phi \rangle = (R^*)^2 \iint_a \phi f(\theta, \phi) \, da(\theta, \phi), \quad (2.9)$$

where the area $a(\theta_c)$ is the area swept when a circle of unit radius is rotated through the angle θ_c ; it includes the coordinates $0 \leq \theta \leq \theta_c$, $-\pi \leq \phi \leq \theta_c$. If the circle rolling process is to be successful in an array of large size we must have $\langle n \rangle > 1$, and $\langle \phi \rangle = 0$. Incorporating these constraints and writing $R^* = 1/(2\tau^*)$, we have

$$L = \iint_a f(\theta, \phi) da(\theta, \phi) > 4\tau^{*2} \quad (2.10)$$

and

$$\langle \phi \rangle = \iint_a \phi f(\theta, \phi) da(\theta, \phi) = 0. \quad (2.11)$$

It follows that

$$\tau_c^* < \tau_o^* = \frac{1}{2} L_o^{1/2} \quad (2.12)$$

where L_o is the maximum value of the integral in (2.10) under the constraint (2.11).

As shown in the Appendix, L is maximized by the choice

$$f(\theta, \phi) = \begin{cases} 1 & da \in a_o(\theta_c) \\ 0 & da \in a_1 = (a - a_o) \end{cases} \quad (2.13)$$

where $a_o(\theta_c)$ (Fig. 4) is the subarea of $a(\theta_c)$ over which $\phi \geq -\phi_o(\theta_c)$, with $\phi_o(\theta_c)$ determined by the condition

$$\int_{-\phi_o}^{\theta_c} \phi \left[\int da(\theta, \phi) \right] = \int_{-\phi_o}^{\theta_c} \phi da(\phi) = 0. \quad (2.14)$$

Hence a limiting configuration is formed by selecting points only from among those found in the limited subarea $R^{*2} a_o(\theta_c)$ of A^* . The limiting value of the critical stress is

$$\tau_o^* = \frac{1}{2} \left[\int_{-\phi_o}^{\theta_c} da(\phi) \right]^{1/2} \quad (2.15)$$

The distribution of forces and segment lengths may be computed from the distribution of points within a_o .

Given the limiting function $\tau_o^*(\theta_c)$, the solution of Eq. (2.15), we may invert to obtain the function $\beta_o(\tau_o^*)$ where

$$\beta_o(\tau_o^*) = \sin\left[\frac{1}{2}\theta_c(\tau_o^*)\right] \quad (2.16)$$

The function $\beta_o(\tau_o^*)$ places a lower bound on the obstacle strength β_c if stable configurations are to exist at stress τ_o^* . Equivalently, it sets a lower bound on the value, β_1 , of the maximum force exerted on the most stable configuration encountered in glide through an array of arbitrarily large size at stress τ_o^* .

Before discussing the detailed properties of the limiting configurations we should perhaps point out that the precise configuration found by a search confined to $R^{*2} a_o(\theta_c)$ depends on the starting point. Since the angle ϕ measured between successive tangents left to right along a configuration differs from that measured right to left a limiting configuration generated right to left across the array will not be strictly identical to one generated left to right. Still another configuration would be formed by searching toward the two lateral

0 0 0 0 4 2 0 1 1 8 3

-13-

boundaries of the array from an interior point. However the physical properties of the limiting configuration (its strength, distribution of forces, and distribution of segment lengths) are uniquely independent of the starting point.

III. PROPERTIES OF THE LIMITING CONFIGURATION

To compute the properties of the limiting configuration we require the function $\phi_o(\theta_c)$, determined by Eq. (2.14). The differential area

$$da(\phi) = \int^{\theta} da(\theta, \phi) \quad (3.1)$$

is

$$da(\phi) = \begin{cases} 1 - \cos(\theta_c - \phi) & 0 \leq \phi \leq \theta_c \\ \cos\phi - \cos(\theta_c - \phi) & \theta_c - \pi \leq \phi \leq 0 \\ \cos\phi + 1 & -\pi \leq \phi \leq \theta_c - \pi \end{cases} \quad (3.2)$$

The function $\phi_o(\theta_c)$ cannot easily be given in closed form, but is plotted in Fig. 5. In the limit of small θ_c

$$\phi_o \rightarrow k_1 \theta_c \quad (3.2)$$

where

$$k_1 = \frac{1}{4} [(3-2\sqrt{2})^{1/3} + (3+2\sqrt{2})^{1/3} - 1] \quad (3.4)$$

$$\cong 0.3388.$$

Given $\phi_o(\theta_c)$ the function $\tau_o^*(\theta_c)$ follows immediately from Eqs. (2.15) and (3.2). The computed function $\tau_o^*(\beta_o)$ is compared to the function $\tau_c^*(\beta_c)$ obtained from computer simulation experiment in Fig. 6. The agreement between the two curves is good over the range $0 \leq \beta \leq 0.7$, which exceeds the range of obstacle strengths which recent theoretical work (Bacon, Kocks, and Scattergood⁸) suggests is physically meaningful. For $\beta > 0.7$ the theoretical curve diverges from that obtained by computer experiment, eventually approaching the limit $\tau_o^* = \sqrt{\pi/2}$ at $\beta_o = 1.0$. This divergence is not surprising since dislocation looping becomes important at high stress, but is not

properly accounted for in the derivation of Eq. (2.15). The problem of "overlap", or indistinguishability of descendants, may also be more serious when τ^* is large.

In the limit of small obstacle strength τ_o^* is given by the relation

$$\begin{aligned} (\tau_o^*)^2 &= \frac{1}{384} (3x^2 + 6x + 13 + 6x^{-1} + 3x^{-2}) \theta_c^3 \\ &\approx 0.7870 (\theta_c/2)^3 \end{aligned} \quad (3.5)$$

where $x = (3+2\sqrt{2})^{1/3}$. This equation may be rewritten

$$(\tau_o^*) = k_2 (\beta_o)^{3/2} = 0.8871 (\beta_o)^{3/2} \quad (3.6)$$

which differs from the Friedel relation (1.3) only through a multiplicative constant. Both the agreement and disagreement between Eqs. (1.3) and (3.6) deserve comment. The agreement in functional form is not fortuitous. Virtually any technique for searching an array by rolling or bowing a circle of radius R^* through a small angle θ_c leads to a search area simple proportional to $(R^*)^2 \theta_c^3$, and will hence yield an equation which differs from (1.3) only through a multiplicative constant. Regarding the disagreement, note that what we have obtained here is an upper bound on the value of τ_c^* in an array of arbitrarily large size, which lies below the Friedel limit by $\sim 11\%$. This result may be possibly questioned on the grounds that τ_o^* also lies below the data obtained from computer simulation (Fig. 6) when β is small. One should, however, recognize that the number of obstacles on the most stable configuration in a finite array is small where τ^* is small and increases with array size n only as \sqrt{n} . Hence the asymptotic relation obtained

from computer simulation in arrays of tractable size will tend to overestimate τ_c^* for an array of infinite size.

The normalized distribution of forces along the limiting configuration may be computed from the relation

$$\rho(\theta, \tau^*) d\theta = R^{*2} \int^{\phi} da(\theta, \phi) \quad (3.7)$$

where $\rho(\theta, \tau^*)$ is the distribution of angles θ , in the limiting configuration at stress τ_o^* . Using Eq. (2.7) and assigning appropriate limits to the integral we obtain

$$\rho(\theta, \tau^*) = \begin{cases} R^{*2} [1 - \cos(\theta + \phi_o)] & \phi_o \leq \pi - \theta_c \\ 2R^{*2} & \theta_c \geq \theta \geq \pi - \phi_o, \phi_o \geq \pi - \theta_c \\ R^{*2} [1 - \cos(\theta + \phi_o)] & \pi - \phi_o \geq \theta \geq 0, \phi_o \geq \pi - \theta_c \end{cases} \quad (3.8)$$

For the range of interest here, $0 \leq \beta_o \leq 0.7$, ϕ_o is less than $(\pi - \theta_c)$ and only the first form is important. Since $\beta = \sin(\theta/2)$,

$$\begin{aligned} \rho(\beta; \tau^*) &= \rho(\theta, \tau^*) d\theta / d\beta \\ &= 2R^{*2} \{ (1 - \beta^2)^{-1/2} [1 - (1 - 2\beta^2) \cos \phi_o] + 2\beta \sin \phi_o \} \end{aligned} \quad (3.9)$$

where we have assumed $\phi_o \leq \pi - \theta_c$. This distribution is, of course, sharply cut off at β_o . It is uniquely fixed by either τ_o^* or β_o since either is sufficient to determine the radius R^* , the angle ϕ_o , and the maximum β_o .

The theoretical distribution (3.9) is compared to computer-generated distributions at $\tau^* = 0.1, 0.3, \text{ and } 0.5$ in Fig. 7. The empirical

distributions were obtained by superimposing the forces found on the most stable configurations in 10 arrays of 10^4 obstacles. The fit seems good. The slight discrepancy near the cut-off value of the theoretical distribution $[\beta_o(\tau_o^*)]$ is due to the fact that the configurations found by the computer have a distribution of β_1 values near β_o .

In the limit of small obstacle strength (or, equivalently, low stress) the density of forces takes the form

$$\rho(\beta; \tau^*) \approx [(\beta/\beta_o) + k_1]^2 / (k_2^2 \beta_o) \quad (\beta < \beta_o \ll 1) \quad (3.10)$$

where k_2 is defined in Eq. (3.6) and k_1 in Eq. (3.4). Note that this limiting distribution can be recast in the form

$$\rho(\beta/\beta_o) \approx [(\beta/\beta_o) + k_1]^2 / k_2^2 \quad (\beta/\beta_o \leq 1, \beta_o \ll 1) \quad (3.11)$$

which is independent of τ^* or β_o . In earlier work³ we deduced that the function $\rho(\beta/\beta_1)$ might be stress-independent. While Eq. (3.9) suggests that this inference is not strictly correct, Eq. (3.11) argues that it becomes correct when τ^* is small. In fact, Eq. (3.9) deviates from its asymptotic form (3.11) by no more than 3% at $\tau_o^* = 0.5$.

Eq. (3.11) is quite accurate over the whole range of interest here.

The normalized distribution of segment lengths, $\rho(l^*, \tau^*)$, may be found by expressing l^* as a function of θ and ϕ and finding the differential subarea of a_o over which l^* is constant. The result is, for $\phi_o \leq \pi - \theta_c$,

$$\rho(l^*, \tau^*) = \begin{cases} l^* \theta_c & 0 \leq l^* \leq l' \\ l^* (\theta_c + \phi_o - 2 \sin^{-1}(l^*/2R)) & l' \leq l^* \leq l'' \end{cases} \quad (3.12)$$

where

$$\begin{aligned} \ell' &= 2R^* \sin(\phi_0/2) \\ \ell'' &= 2R^* \sin((\theta_c + \phi_0)/2) \end{aligned} \quad (3.13)$$

The mean segment length, $\langle \ell(\tau^*) \rangle$, is the quantity which is usually compared to the Friedel relation (1.5). Using Eq. (3.12),

$$\begin{aligned} \langle \ell(\tau^*) \rangle &= \int_0^{\ell''} \ell^* \rho(\ell^*; \tau^*) d\ell \\ &= (2/3) (2R^*)^3 \left\{ \cos(\phi_0/2) \left[1 - \frac{1}{3} \cos^2(\phi_0/2) \right] \right. \\ &\quad \left. - \cos\left(\frac{\theta_c + \phi_0}{2}\right) \left[1 - \frac{1}{3} \cos^2\left(\frac{\theta_c + \phi_0}{2}\right) \right] \right\} \end{aligned} \quad (3.14)$$

The calculated function $\langle \ell(\tau^*) \rangle$ is compared to the function $\langle \ell(\tau^*) \rangle$ obtained through computer simulation in Fig. 8. The empirical curve was found by averaging the segment lengths along the most stable configuration in each of ten arrays of 10^4 obstacles at each value of τ^* for which a data bar is shown. The calculated curve closely fits the empirical data. Both curves lie below the prediction of the Friedel model. When τ^* or θ_c is small $\langle \ell(\tau^*) \rangle$ is approximated by the asymptotic relation

$$\begin{aligned} \langle \ell(\tau^*) \rangle &\sim \frac{1}{6} \bar{k}_2^{-3} [(1+k_1)^4 - k_1^4] (\theta_c/2)^{-1/2} \\ &= 0.764 (\theta_c/2)^{-1/2} \\ &= 0.734 (\tau^*)^{-1/3} \end{aligned} \quad (3.15)$$

which suggests that the Friedel relation overestimates the asymptotic $\langle \ell(\tau^*) \rangle$, by about 33%. The two relations are, however, identical in functional form.

While the model developed here yields an excellent fit to the mean segment length $\langle \ell(\tau^*) \rangle$, it is less successful in matching the distribution of segment lengths. The density function $\rho(\ell^*, \tau^*)$ calculated from Eq. (3.12) is compared to that obtained from computer simulation in Fig. 9. The empirical curve was determined by compiling the segment lengths found along the most stable configuration in each of 10 arrays of 10^4 points at $\tau^* = 0.1$. The calculated curve correctly predicts that $\rho(\ell^*)$ is zero when ℓ^* is significantly larger than $\langle \ell \rangle$, hence over most of the available range $0 < \ell^* < 2R^*$. However, the theoretical curve does not correctly reproduce the shape of the empirical distribution. It is not clear whether this discrepancy principally results from the approximations involved in the theoretical model or from the finite size of the arrays used to generate the empirical distribution.

ACKNOWLEDGEMENTS

The authors are grateful to Dale H. Klahn for helpful discussions during the formulation of this problem. This work was supported by the Atomic Energy Commission through the Inorganic Materials Research Division of the Lawrence Berkeley Laboratory.

REFERENCES

1. J. W. Morris, Jr. and Dale H. Klahn, J. Appl. Phys. 44, 4882 (1973).
2. J. W. Morris, Jr. and C. K. Syn, J. Appl. Phys. 45, 961 (1974).
3. J. W. Morris, Jr. and Dale H. Klahn, J. Appl. Phys. 45, 2027 (1974).
4. J. Friedel, Dislocations (Addison-Wesley, Reading, Mass., 1969) p. 224.
5. P. L. Fleischer and W. R. Hibbard, in The Relation Between the Structure and Mechanical Properties of Metals (H. M. Stationary Office, London, 1963) p. 262.
6. A. J. E. Foreman and M. J. Makin, Phil. Mag. 14, 911 (1966).
7. W. Feller, An Introduction to Probability Theory and its Applications, 2nd ed., (Wiley, New York, 1957) Vol. I.
8. D. J. Bacon, U. F. Kocks, and R. O. Scattergood, Philos. Mag. 28, 1241 (1973).

APPENDIX

We wish to choose $f(\theta, \phi)$ such that the integral

$$L = \iint_a f(\theta, \phi) da(\theta, \phi) \quad (\text{A.1})$$

is maximized subject to the constraints

$$f(\theta, \phi) \leq 1 \quad (\text{A.2})$$

$$\iint_a \phi f(\theta, \phi) da(\theta, \phi) = 0 \quad (\text{A.3})$$

where a is the search area of Fig. 2, defined by $0 \leq \theta \leq \theta_c$, $-\pi \leq \phi \leq \theta_c$.

The solution is

$$f(\theta, \phi) = \begin{cases} 1 & da \in a_0 \\ 0 & da \in a_1 = (a - a_0) \end{cases} \quad (\text{A.4})$$

where a_0 is the subarea defined by $0 \leq \theta \leq \theta_c$, $-\phi_0 \leq \phi \leq \theta_c$, with ϕ_0 determined by the condition

$$\int_{-\phi_0}^{\theta_c} \phi \left[\int_0^{\theta_c} da(\theta, \phi) \right] = \int_{-\phi_0}^{\theta_c} \phi da(\phi) = 0 \quad (\text{A.5})$$

The proof is straightforward. Let $q(\theta, \phi)$ be a piece-wise continuous function, $0 \leq q \leq 1$ such that

$$f(\theta, \phi) = \begin{cases} 1 - q(\theta, \phi) & da \in a_0 \\ q(\theta, \phi) & da \in a_1 \end{cases} \quad (\text{A.6})$$

and define

$$L_0 = \iint_{a_0} da(\theta, \phi). \quad (\text{A.7})$$

Then

$$L - L_0 = \Delta L = J_1 - J_0 \quad (\text{A.8})$$

where

$$J_i = \iint_{a_i} q \, da \geq 0 \quad (\text{A.9})$$

From Eqs. (A3) and (A5)

$$K_1 = K_0, \quad (\text{A.10})$$

$$K_1 = \iint_{a_1} (-\phi) q \, da. \quad (\text{A.11})$$

It follows from the mean value theorem and the condition

$\phi_0 \leq (-\phi) \leq \pi$ in a_1 , that

$$K_1 = (\phi_0 + N)J_1 \quad (\text{A.12})$$

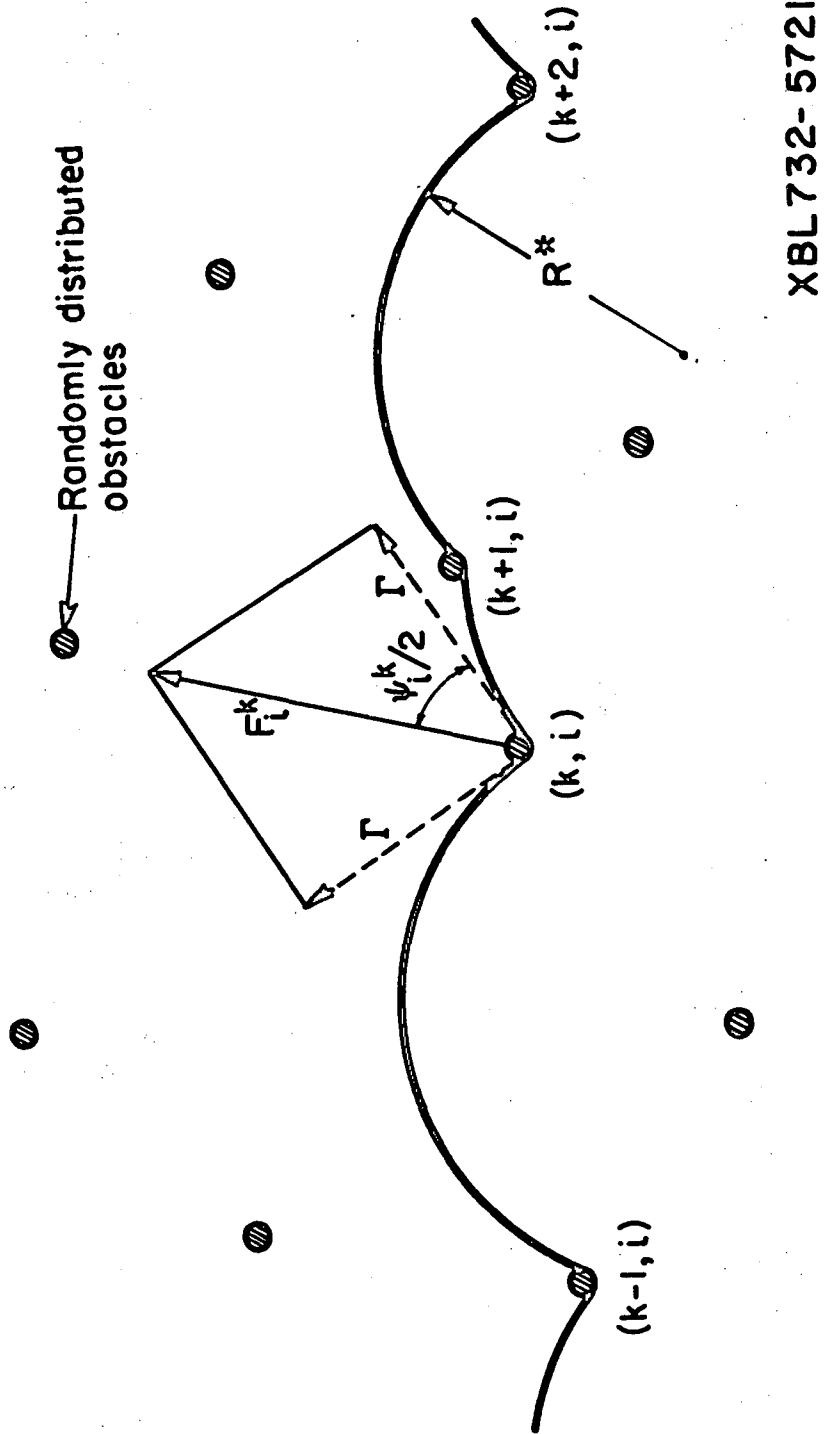
where $N \geq 0$. Similarly,

$$K_0 = (\phi_0 - M)J_0 \quad (\text{A.13})$$

where $M \geq 0$. Equations (A10) and (A9) then require that $M \leq \phi_0$ and

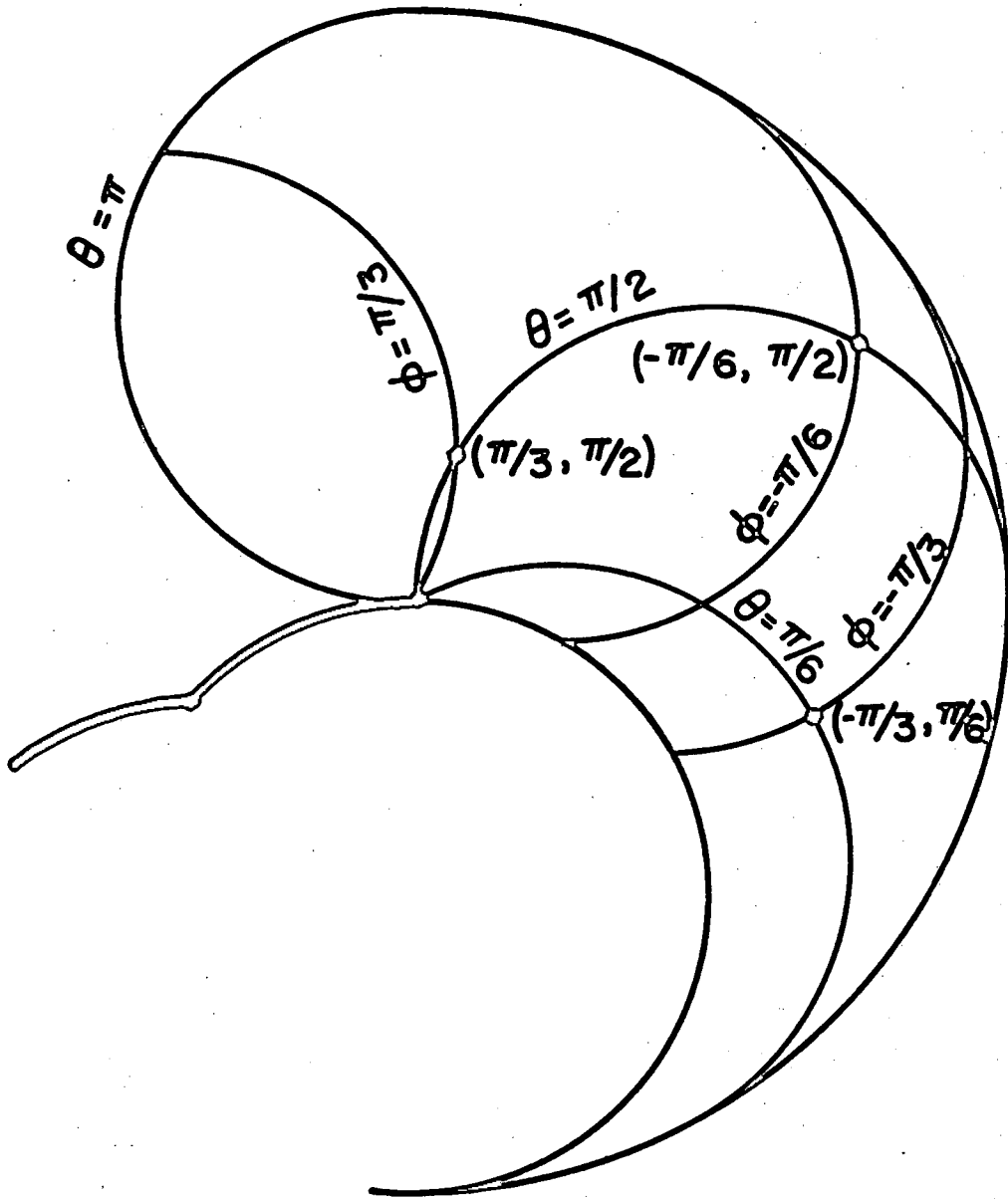
$$J_1 = \left[\frac{\phi_0 - M}{\phi_0 + N} \right] J_0 \leq J_0 \quad (\text{A.14})$$

Hence $\Delta L \leq 0$ for arbitrary $q(\theta, \phi)$. The equality holds only if $q = 0$, which establishes Eq. (A4).



XBL732-5721

Figure 1. Detail of mechanical equilibrium in the i^{th} obstacle configuration.



XBL 748-6938

Figure 2. Parametrization of the area searched by circle-rolling to an angle $\theta_c = \pi$.

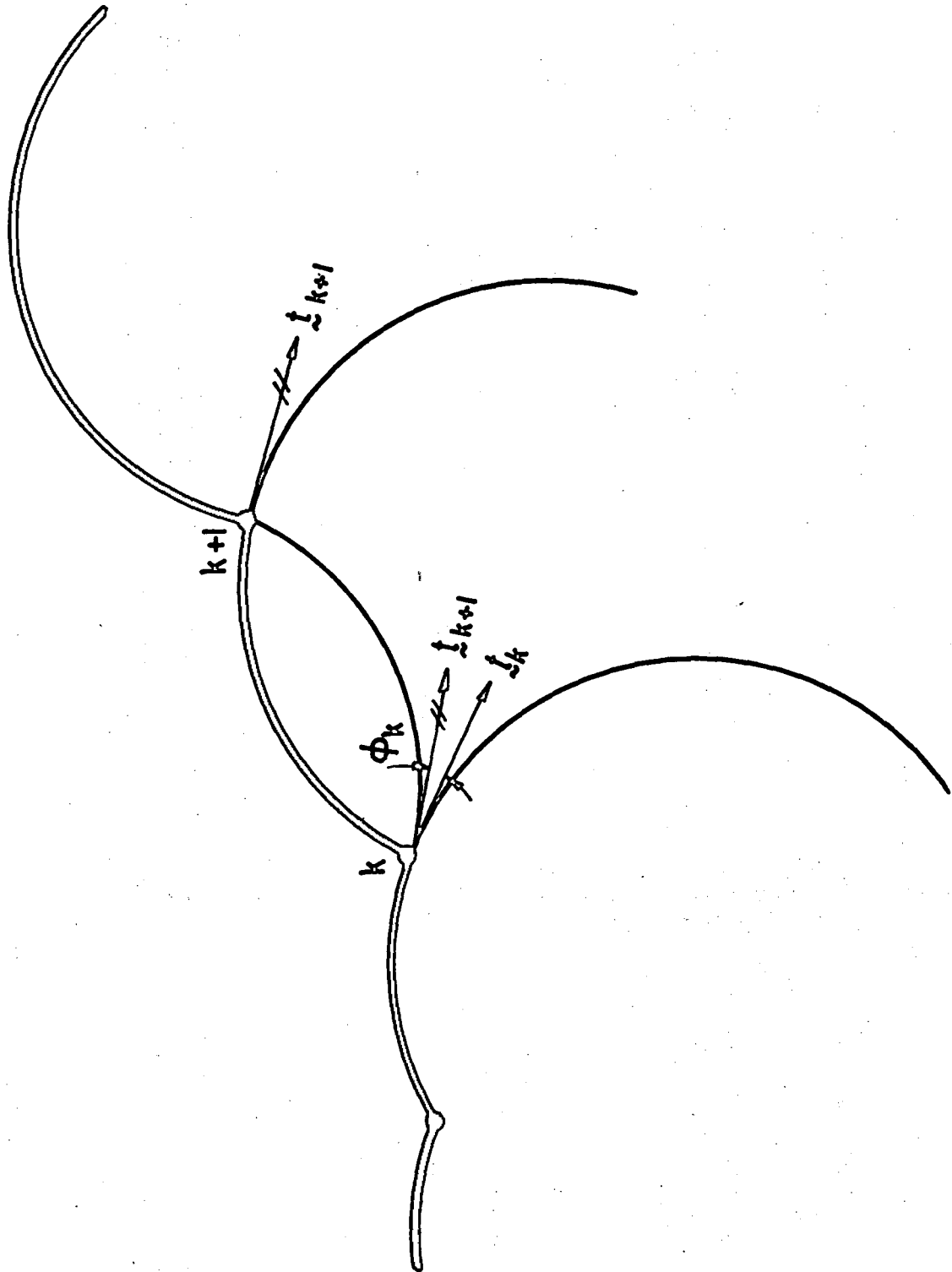
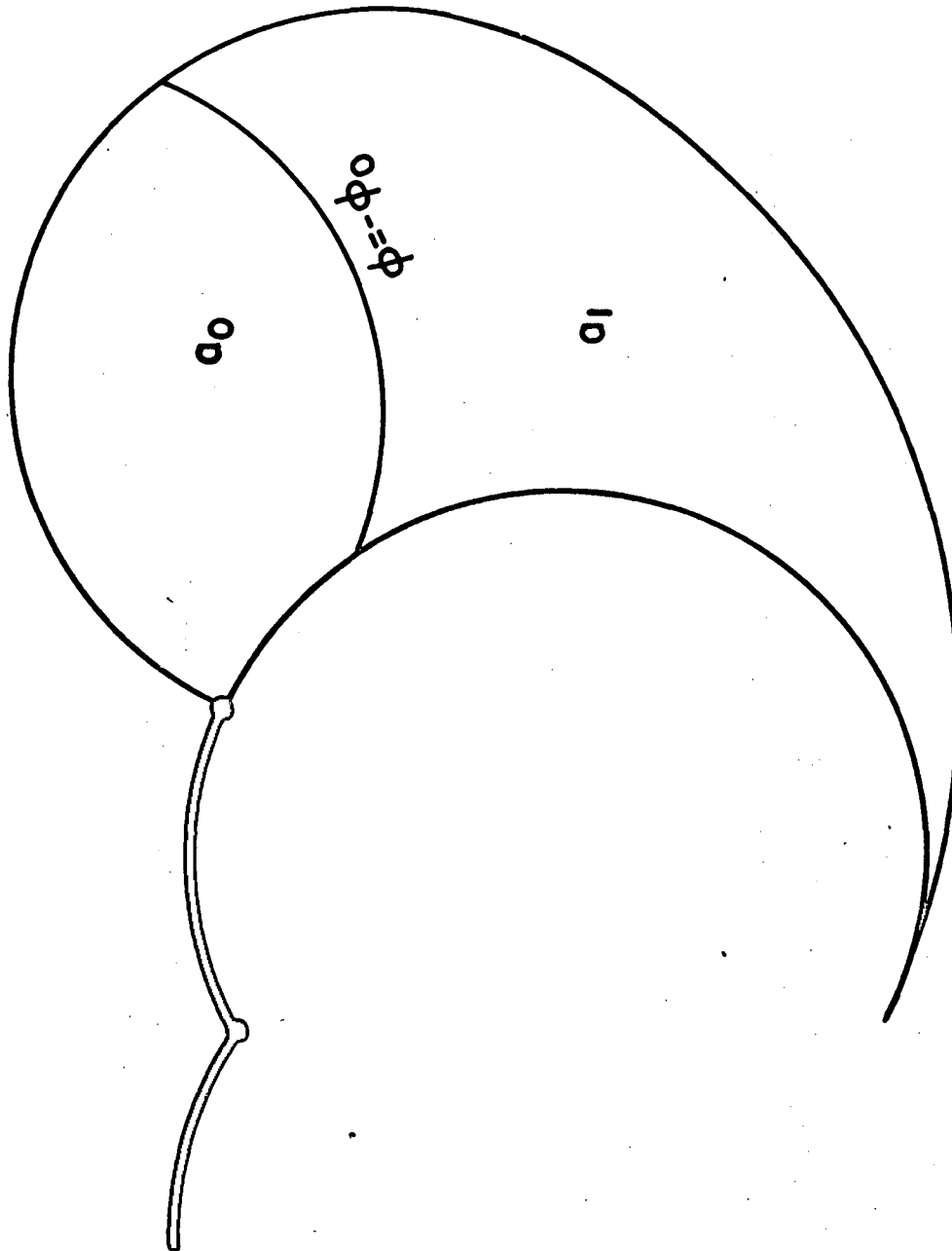
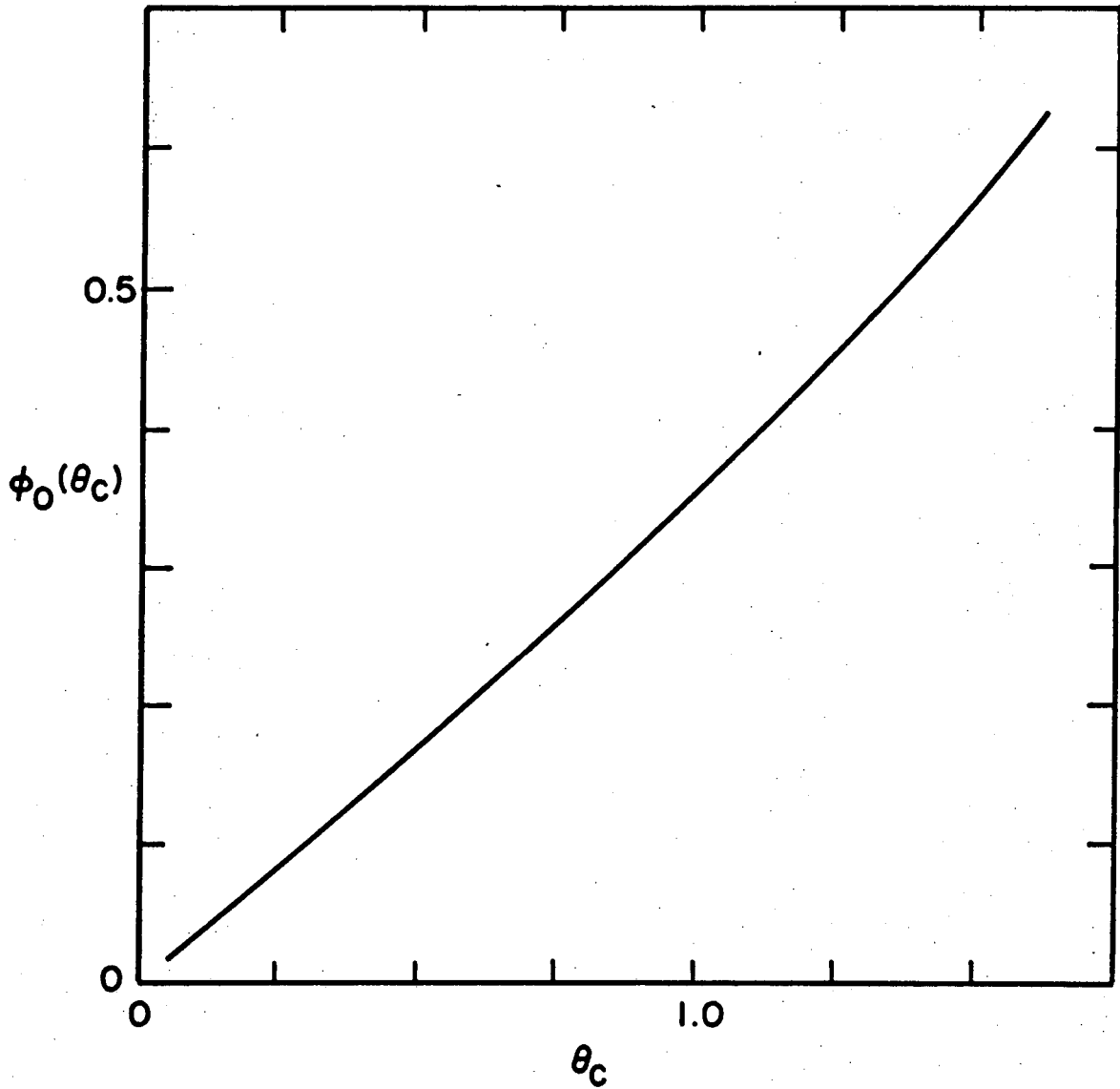


Figure 3. Diagram illustrating that the angle ϕ_k measures the change in direction of the dislocation line at obstacle $(k + 1)$.



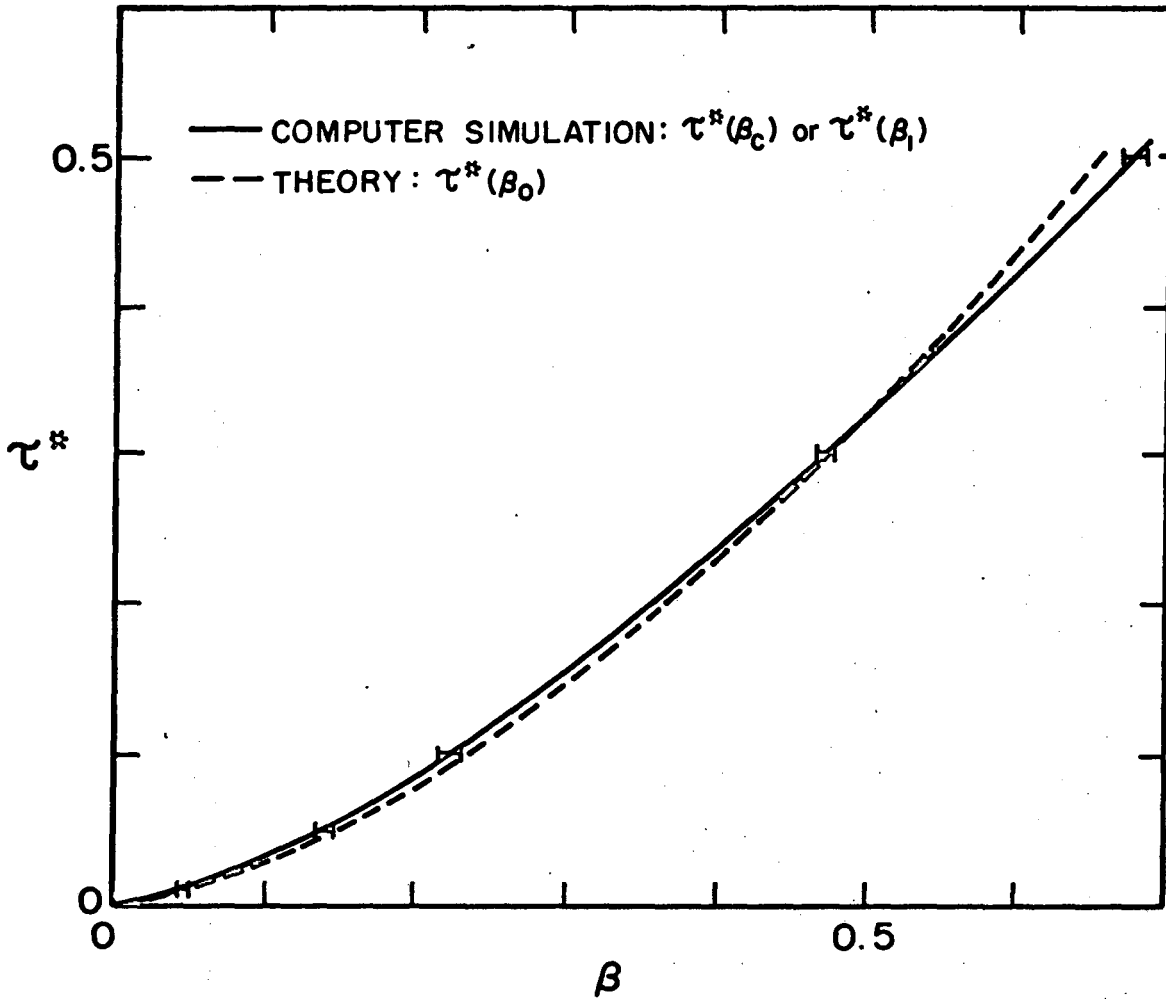
XBL 748-6940

Figure 4. Division of the search area (a) into the limiting area (a_0) and the excess area (a_1) by the coordinate line $\phi = -\phi_0$.



XBL 748 - 6941

Figure 5. The limiting parameter $\phi_0(\theta_c)$.



XBL 748-6942

Figure 6. The limiting stress $\tau_0(\beta_0)$ compared to the function $\tau^*(\beta_1)$ obtained by direct computer simulation of glide through arrays of 10^4 obstacles. The bars include the values of the maximum force (β_1) in the most stable configuration encountered in glide through each of ten arrays of 10^4 points at each value of the stress τ for which a data bar is shown.

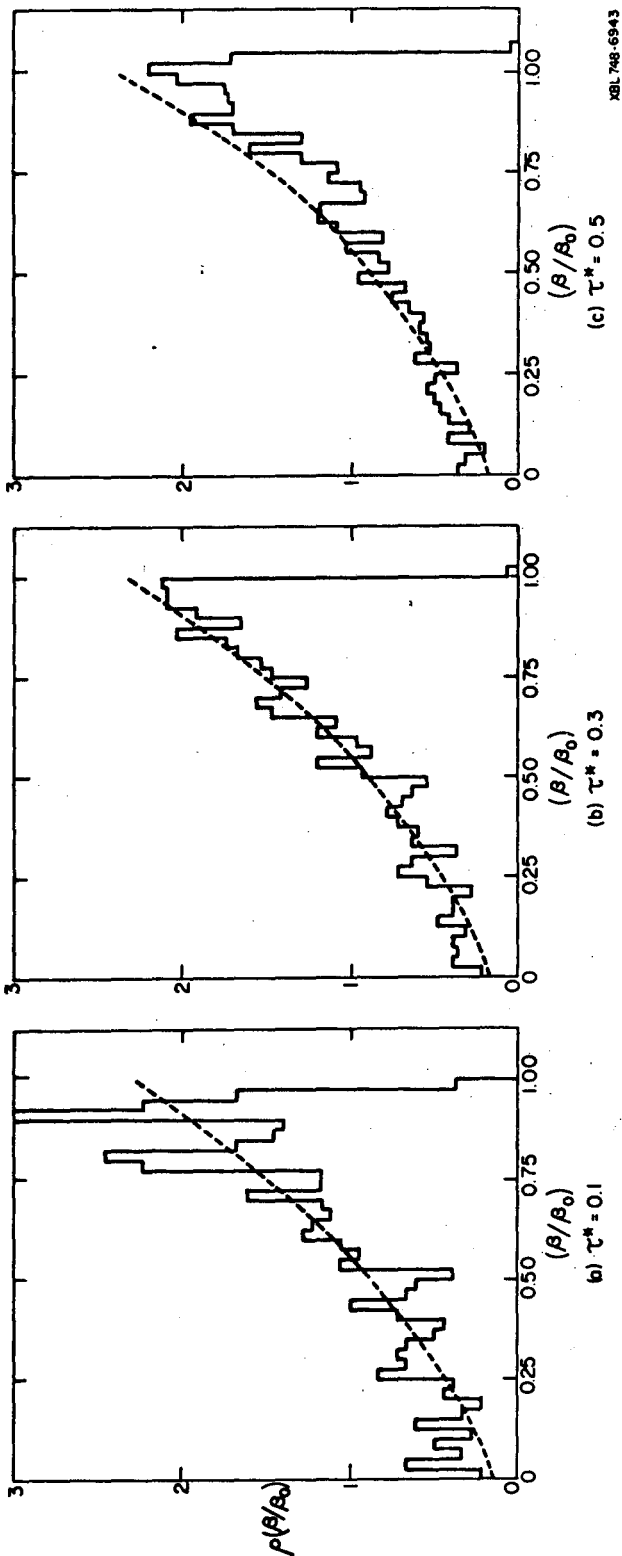
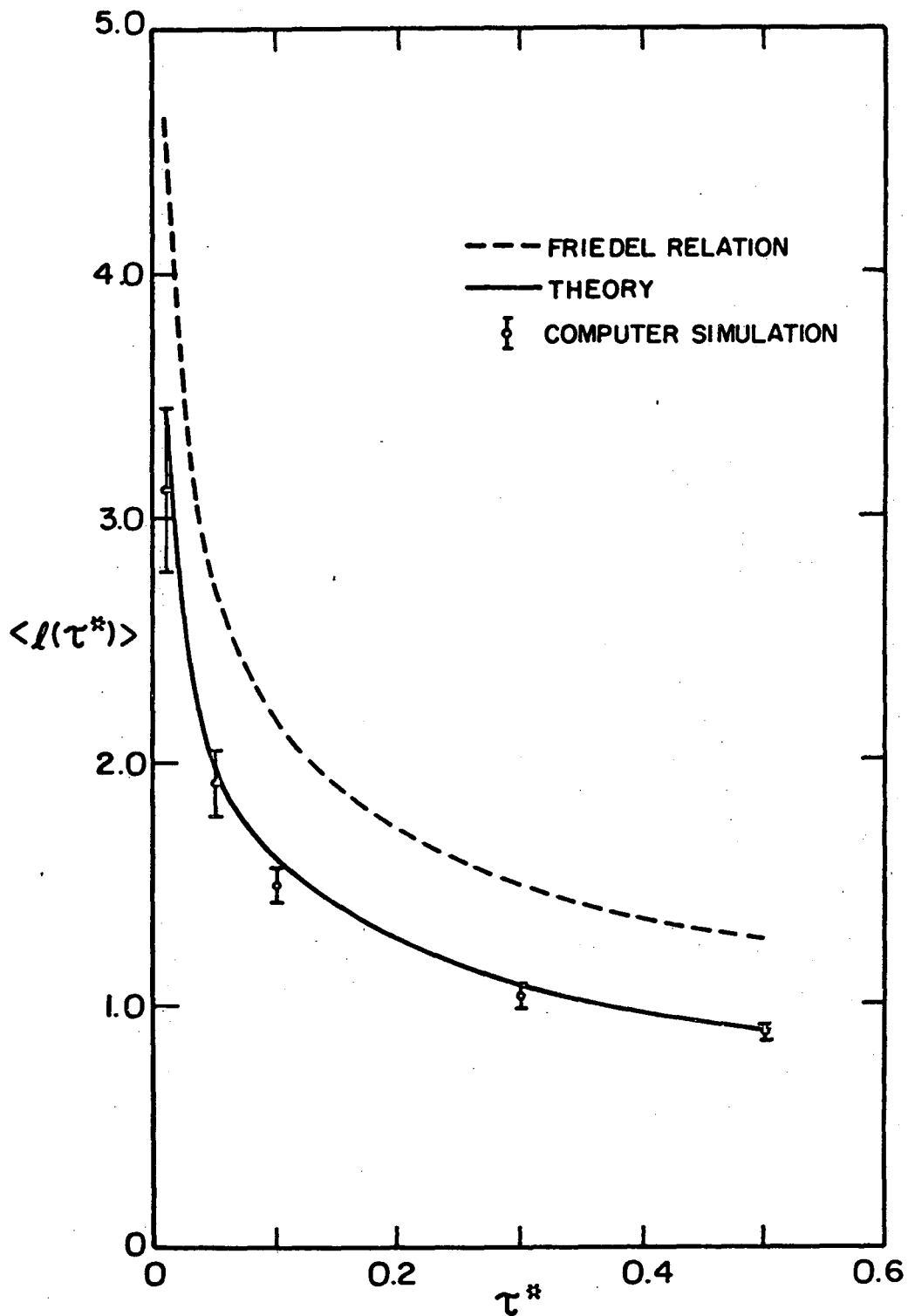
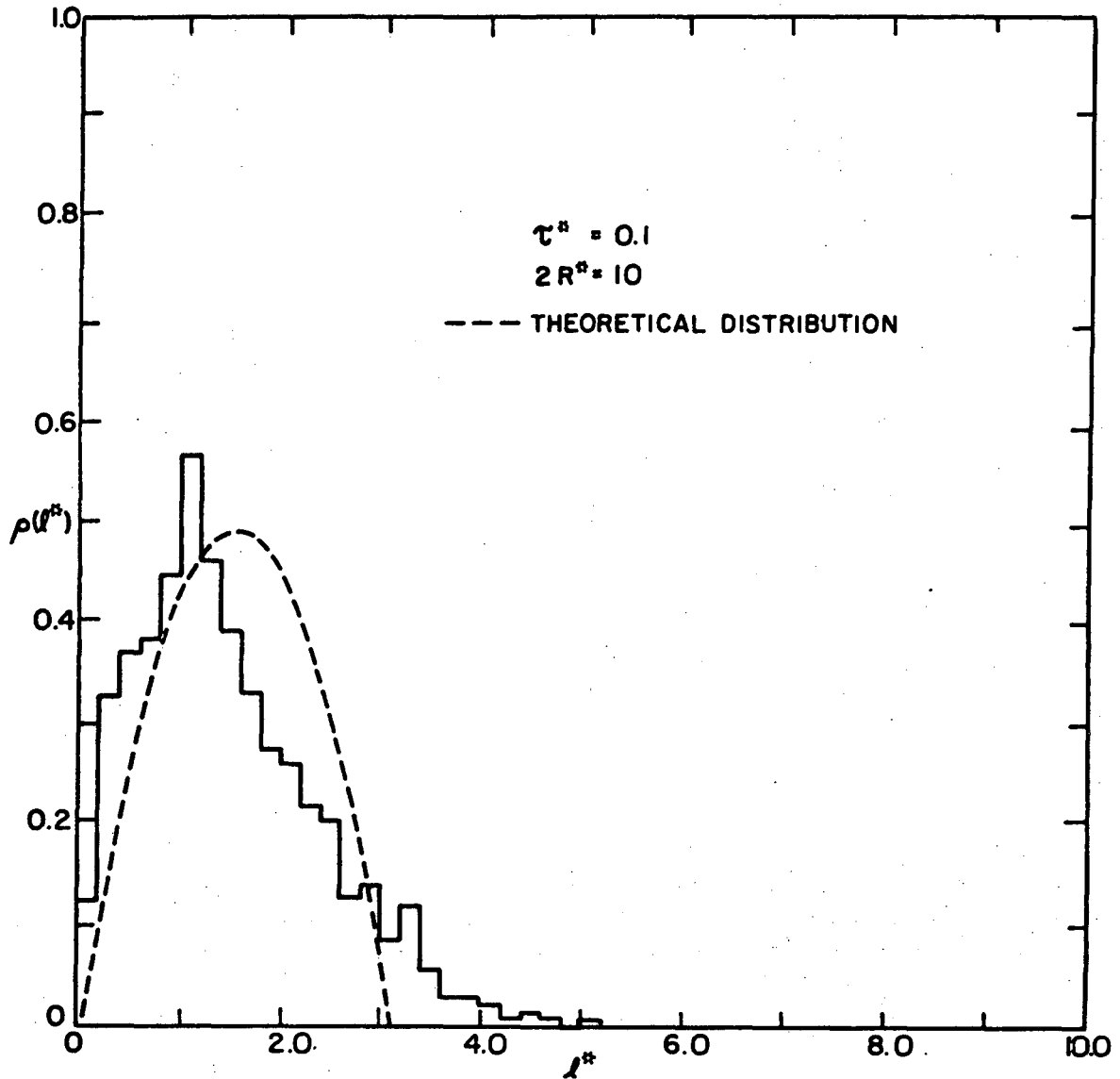


Figure 7. The distribution of forces in the limiting configuration compared to histograms obtained through direct computer simulation of glide through arrays of 10^4 points. The limiting forces (β_0) are: $\beta_0 = 0.2322$ at $\tau = 0.1$, $\beta_0 = 0.4751$ at $\tau = 0.3$, $\beta_0 = 0.6526$ at $\tau = 0.5$.



XBL 748-6944

Figure 8. The mean segment length $\langle l(\tau^*) \rangle$ in the limiting configuration compared to that predicted by the Friedel relation (eq. 1.5) and that determined by direct computer simulation of glide through arrays of 10^4 points. The data bars include the mean segment length in the most stable configuration in each of ten arrays of 10^4 points at each value of the stress for which a data bar is shown.



XBL 748-6945

Figure 9. The distribution of segment lengths in the limiting configuration at $\tau^* = 0.1$ compared to a histogram determined by direct computer simulation of dislocation glide through arrays of 10^4 points at $\tau^* = 0.1$. The mean segment length $\langle l^* \rangle$ is 1.572 in the limiting distribution compared to 1.493 for the histogram.

LEGAL NOTICE

This report was prepared as an account of work sponsored by the United States Government. Neither the United States nor the United States Atomic Energy Commission, nor any of their employees, nor any of their contractors, subcontractors, or their employees, makes any warranty, express or implied, or assumes any legal liability or responsibility for the accuracy, completeness or usefulness of any information, apparatus, product or process disclosed, or represents that its use would not infringe privately owned rights.

TECHNICAL INFORMATION DIVISION
LAWRENCE BERKELEY LABORATORY
UNIVERSITY OF CALIFORNIA
BERKELEY, CALIFORNIA 94720